Competition between orthorhombic and re-entrant tetragonal phases in underdoped $Ba_{1-x}K_{x}Fe_{2}As_{2}$ probed by the response to controlled disorder

E. I. Timmons, M. A. Tanatar, K. Willa, S. Teknowijoyo, Kyuil Cho, M. Kończykowski, O. Cavani, Yong Liu, T. A. Lograsso, U. Welp, and R. Prozorov

Phys. Rev. B **99**, 054518 — Published 26 February 2019

DOI: 10.1103/PhysRevB.99.054518

Competition between orthorhombic and re-entrant tetragonal phases in underdoped $Ba_{1-x}K_xFe_2As_2$ probed by the response to controlled disorder

E. I. Timmons,[1,2] M. A. Tanatar,[1,2,*] K. Willa,[3] S. Teknowijoyo,[1,2] Kyuil Cho,[1] M. Kończykowski,[4] O. Cavani,[4] Yong Liu,[1] T. A. Lograsso,[1,5] U. Welp,[3] and R. Prozorov[1,2,†]

[1]*Ames Laboratory US DOE, Ames, Iowa 50011, USA*
[2]*Department of Physics and Astronomy, Iowa State University, Ames, Iowa 50011, USA*
[3]*Materials Science Division, Argonne National Laboratory, 9700 S. Cass Avenue, Argonne, Illinois 60439, USA*
[4]*Laboratoire des Solides Irradiés, École Polytechnique, CNRS, CEA, Université Paris-Saclay, 91128 - Palaiseau Cedex, France*
[5]*Department of Materials Science and Engineering, Iowa State University, Ames, Iowa 50011, USA*

(Dated: January 7, 2019)

Low-temperature (22 K) irradiation with 2.5 MeV electrons, creating point defects affecting elastic scattering, was used to study the competition between stripe C_2 and tetragonal C_4 antiferromagnetic phases which exist in a narrow doping range around x =0.25 in hole-doped $Ba_{1-x}K_xFe_2As_2$. In nearby compositions outside of this range, at x =0.22 and x =0.19, the temperatures of both the concomitant orthorhombic/stripe antiferromagnetic transition T_{C2} and the superconducting transition T_c are monotonically suppressed by added disorder at similar rates of about 0.1 K/$\mu\Omega$cm, as revealed through using resistivity variation as an intrinsic measure of scattering rate. In a stark contrast, a rapid suppression of the C_4 phase at the rate of 0.24 K/$\mu\Omega$cm is found at x =0.25. Moreover, this suppression of the C_4 phase is accompanied by unusual disorder-induced stabilization of the C_2 phase, determined by resistivity and specific heat measurements. The rate of the C_4 phase suppression is notably higher than the suppression rate of the spin-vortex phase in the Ni-doped $CaKFe_4As_4$ (0.16 K/$\mu\Omega$cm).

Cooper pair binding mediated by magnetic fluctuations[1] is actively discussed as a possible mechanism of superconductivity in several classes of unconventional superconductors including heavy fermions[2], high-T_c cuprates[3] and, more recently, iron-based superconductors[4]. A fingerprint of this model is the observation of the highest superconducting transition temperature, T_c, coinciding with a quantum critical point (QCP) where the temperature of the magnetic transition, T_N, goes to zero at a point in a $T-x$ phase diagram with x being a non-thermal control parameter such as doping, pressure, magnetic field or disorder[1,5,7]. Strong magnetic fluctuations at the QCP lead to non-Fermi liquid behavior of all electronic properties, for example logarithmic divergence of the heat capacity and T-linear electrical resistivity[5,6].

In iron-based superconductors, this phenomenology is clearly observed in isovalent P-substituted $BaFe_2(As_{1-x}P_x)_2$ (Ba122)[8–10], however it fails in hole-doped $Ba_{1-x}A_xFe_2As_2$ (A=Na,K) compositions which have the highest T_c. Here, the suppression of the transition temperature T_{C2} of the orthorhombic antiferromagnetic phase with stripe pattern of in-plane moments (C_2 phase)[11,12] does not proceed monotonically to zero, but is interrupted by the emergence of a new tetragonal C_4 magnetic phase below temperature T_{C4}[13–18]. Being in very close proximity to the highest T_c doping range, this phase may play an important, yet not understood, role in the superconducting pairing[19].

The C_4 phase is also observed in other hole-doped 122-type compounds, $Ca_{1-x}Na_xFe_2As_2$[20], $Sr_{1-x}Na_xFe_2As_2$[21] and $Ba(Fe_{1-x}Mn_x)_2As_2$[22]. The C_4 phase in $Sr_{1-x}Na_xFe_2As_2$ was shown to be a double-Q spin-charge density wave, with a moment equal to zero on every second iron atom[23]. A similar C_4 phase but with a different type of magnetic order is found in electron-doped $CaK(Fe_{1-x}TM_x)_2As_2$, with TM=Co, Ni[24]. Theoretically, the origin of this phase has been attributed to itinerant magnetism[25,26], magnetic moments with effects of frustration[27] or the effects of spin-orbit coupling[28,29].

It was recently suggested, that disorder can lead to a stabilization of the spin-charge density wave C_4 phase as compared to the C_4 spin vortex state and the C_2 phase in the phase diagram of the hole-doped compositions[30]. Motivated by this theoretical prediction, we report here a study on the effect of electron irradiation in hole-doped $Ba_{1-x}K_xFe_2As_2$ with x =0.25 revealing clear signatures of the C_4 phase in temperature-dependent resistivity and heat capacity measurements. For reference, we also study the effect of electron irradiation on nearby compositions with x =0.19 and x =0.22 outside the C_4 phase doping range. We find that disorder suppresses the C_4 phase at a rate which is significantly higher than the suppression rate of the C_2 phase in nearby compositions and in the spin-vortex phase of $CaK(Fe_{1-x}Ni_x)_4As_4$[31]. It also leads to an unusual slight increase of T_{C2} suggesting its stabilization with disorder. Our results clearly show competition between these two types of magnetic orders.

Single crystals of $Ba_{1-x}K_xFe_2As_2$ were grown as described in detail in Ref. 32. Large, above 5×5 mm^2 surface area crystals were cleaved on both sides to a thick-

* tanatar@ameslab.gov
† prozorov@ameslab.gov

ness of typically 0.1 mm to minimize the variation of the K-content with thickness. The cleaved slabs were characterized by electron-probe microanalysis with wavelength dispersive spectroscopy (WDS). The crystals from three different batches were used with WDS compositions determined as x=0.19, 0.22 and 0.25. The large slabs were cleaved into bars for four-probe resistivity measurements so that all samples were originating from the same slab of the crystal. Samples typically had a size of 2×0.5×0.1 mm^3 and long and short sides corresponding to the crystallographic a-axis and c-axis, respectively. Low-resistance contacts to the samples were made by soldering Ag wires with tin[33,34]. The contacts were found to be both mechanically and electronically stable under electron irradiation. Four-probe resistivity measurements were performed in a *Quantum Design* PPMS. Specific heat was measured in a helium cryostat by using an AC calorimeter built on SiN membrane chips at frequencies in the 1 Hz range as described in Refs.[35,36].

For our study we selected samples with the sharpest features in the temperature-dependent resistivity $\rho(T)$ at concomitant tetragonal/orthorhombic and paramagnetic/C_2 antiferromagnetic transitions in samples x =0.19 and 0.22. The largest problem however is finding samples with sharp features at the C_2 to C_4 transition for x =0.25 which is extremely sensitive to sample to sample variation without detectable composition variations with Δx ∼0.003. We therefore did all pre-characterization of the samples with resistivity and only performed specific heat on selected samples.

The samples for resistivity measurements during and after electron irradiation were mounted on a thin mica plate in a hollow *Kyocera* chip, so that they could be moved between the irradiation chamber and the resistivity setup (in a different ^{4}He cryostat) without disturbing the contacts. The low-temperature 2.5 MeV electron irradiation was performed at the SIRIUS Pelletron linear accelerator operated by the *Laboratoire des Solides Irradiés* (LSI) at the *Ecole Polytechnique* in Palaiseau, France[37]. The *Kyocera* chip was mounted inside the irradiation chamber and was cooled by a flow of liquid hydrogen to $T \approx 22$ K in order to remove excess heat produced by relativistic electrons upon collision with the ions. The flux of electrons amounted to about 2.7 μA of electric current through a 5 mm diameter diaphragm. This current was measured with the Faraday cup placed behind a hole in the sample stage, so that only transmitted electrons were counted. The irradiation rate was about 5×10^{-6} C/(cm^2·s) and large doses were accumulated over the course of several irradiation runs. Throughout the manuscript we use "pristine" and "unirradiated" interchangeably to describe samples that were not exposed to electron radiation.

Three samples selected A,B and C had sharp maximums in temperature-dependent resistivity derivatives at T_{C4} equal 33, 25 and 35 K, and minimums at T_{C2} 60 and 56.3 K, respectively. A selected sample A of x =0.25 composition was irradiated multiple times adding doses in small steps and tracking the fine evolution of its temperature-dependent resistivity to determine T_{C2}, T_{C4} and the superconducting T_c. The sample was extracted from the irradiation chamber following each irradiation dose step and its temperature-dependent resistivity was measured *ex-situ* after annealing at room temperature. This annealing, however, does not remove residual disorder, so that the sample resistance gradually increased in successive runs. A second sample B with slightly higher T_{C4} ∼35 K suggesting somewhat higher K-content was mounted on the same chip and underwent the same irradiation procedure, however, was not measured in the intermediate steps. After an accumulation of a significant dose and the ensuing characterization by resistivity which produced results that were qualitatively consistent with sample A (we found slight increase of T_{C2} by about 2 K), a small piece (100μm × 160μm) was cut from the area between potential contacts to be used for microcalorimetric measurements. Another pristine sample C, having identical T_{C4} and T_{C2} and thus composition with sample B, was measured as a reference sample in specific heat apparatus. The samples of other compositions x =0.19 and x =0.22 were irradiated without intermediate measurements, receiving the maximum dose in one run.

In Fig. 1 we show the temperature-dependent resistivity of selected samples with x=0.19, 0.22 and 0.25 in the pristine state before irradiation. The room-temperature resistivity of the samples was set to 300 $\mu\Omega$cm, the statistically significant value as determined on a big array of crystals[32]. The actually measured values for the individual samples were within the 10% uncertainty of the geometric factor determination. The $\rho(T)$ curves show the typical behavior of hole-doped $Ba_{1-x}K_xFe_2As_2$[32,38], with a broad crossover at around 200 K. Samples with x=0.19 and x =0.22 show a small acceleration of resistivity decrease on cooling through T_{C2} and a rather sharp superconducting transition at T_c. The T_{C2} feature is most clearly seen as a sharp feature in the temperature derivative of the resistivity, $d\rho/dT$, top right panel of Fig. 1. The $\rho(T)$ of the sample with x =0.25 shows slight step up at T_{C2}, leading to a sharp minimum in resistivity derivative. The resistivity of the samples just above T_c decreases monotonically with x from about 40 $\mu\Omega$cm in x =0.19 to 30 $\mu\Omega$cm in x =0.25 and the residual resistivity ratios increase from about 7 to 10, respectively. The T_{C2} feature is shifting down in temperature with increasing x reaching T_{C2} =60 K for x =0.25 (the same feature in samples B and C is observed at 56.5 K in resistivity and at 57.4 K in heat capacity (sample C) indicating its bulk nature, see Fig. 3a below). In the bottom panel of Fig. 1 we plot the characteristic temperatures as determined from resistivity measurements (circles T_{C2}, open up-triangles T_c as determined from offset criterion) as a function of x in comparison with the phase diagram by Böhmer *et al.*[15] (lines in the figure). The position of the x =0.25 sample on this phase diagram does not follow T_{C2} line. However, if we allow for a small variation of x for our x =0.25 WDS sample to match T_{C2} with the value reported by Böhmer, we simultaneously match the T_{C4} feature (red solid square) as well. The composition

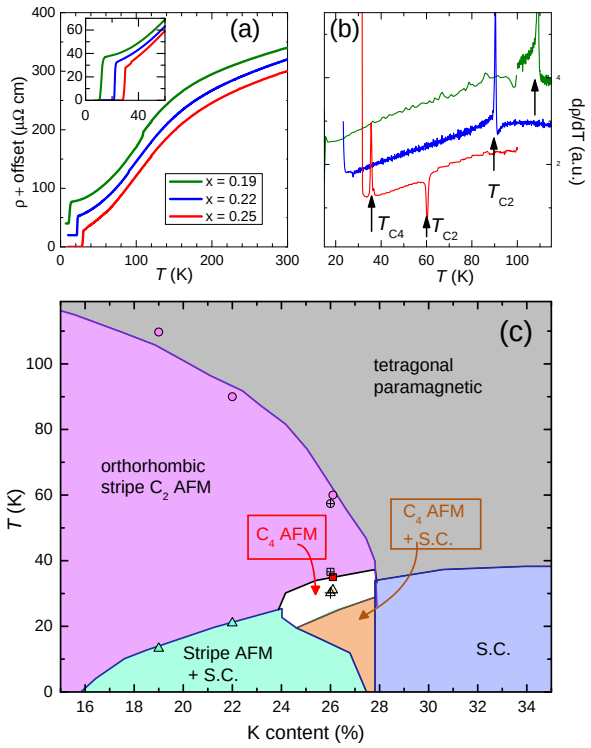

FIG. 1. (Color Online) (a) Temperature-dependent resistivity of selected samples of $Ba_{1-x}K_xFe_2As_2$, x =0.19 (green), 0.22 (blue) and 0.25 (red), the curves are offset vertically. Inset: low temperature region showing differences in the superconducting transition temperatures and resistivity values at T_c. (b) Resistivity derivative, revealing a sharp feature at the structural transitions at T_{C2} and T_{C4}. (c) Doping phase diagram of $Ba_{1-x}K_xFe_2As_2$ in the range of C_4 phase formation, as proposed by Böhmer et al.[15] (lines). The positions of C_2 (circles), C_4 (square) and superconducting (triangle) transitions for samples with x =0.19 and x =0.22 are matching well with the diagram, but the position of x =0.25 sample was adjusted to 0.264 to match the C_2 line with the concomitant match of the C_4 line. Symbols with crosses show the positions of the features in the heat capacity measurements, see Fig. 3 below.

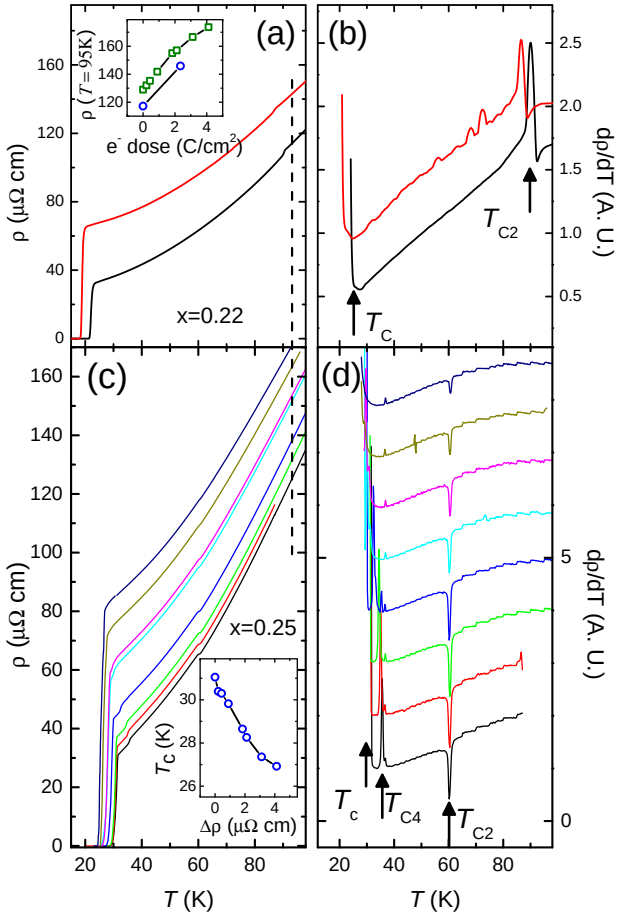

FIG. 2. (Color Online) Temperature-dependent resistivity (left panels) and resistivity derivative (right panels) of $Ba_{1-x}K_xFe_2As_2$ with x =0.22 (top) and x =0.25 (bottom). Black curves in panels (a) and (b) are for pristine x =0.22 sample, red curves are for sample after electron irradiation with 2.35 C/cm^2. Panels (c) and (d) show systematics of the evolution of the temperature-dependent electrical resistivity in sample with x = 0.25 with irradiation, bottom to top: pristine sample (black), 0.212 C (red), 0.438 C (green), 0.893 C (blue), 1.835 C (cyan), 2.115 C (magenta), 3.115 C (dark yellow), 4.115 C (navy). Inset in panel (a) shows resistivity at 95 K as a function of electron irradiation dose for sample with x =0.22 (blue) and x =0.25 (green). Inset in panel (c) shows the evolution of the superconducting transition temperature in sample with x =0.25 as a function of the change of resistivity at 95 K, above T_{C2}.

difference amounts to approximately 1%, which is presumably coming from the difference in calibrations in the composition analysis between WDS (our case) and EDX (as used by Böhmer *et al.*[15]). The onset of the resistive transition to superconducting phase in samples A and B (not shown) occurs at 30 K with no indication of the T_c depression reported in[15].

In Fig. 2 we show the evolution of the temperature-dependent resistivity $\rho(T)$ with electron irradiation. The irradiation increases the resistivity of the samples, with the increase being nearly temperature independent above T_{C2}, but strongly temperature-dependent below. This difference in response to controlled disorder above and below T_{C2} is found in other $BaFe_2As_2$ based materials, P-doped[39], Ru-doped[40,41] and K-doped[42,43]. Since the resistivity above T_{C2} roughly obeys Matthiessen rule, we used the post-irradiation increase of resistivity at set temperature T=95 K (dashed lines in left panels in Fig. 2) as an intrinsic measure of disorder. The electron dose-dependence of the resistivity for samples x =0.22 (blue circles) and x =0.25 (green squares) is shown in the inset in the top left panel of Fig. 2.

Irradiation suppresses T_{C2} in samples with x =0.19 (not shown) and x =0.22 (top right panel of Fig. 2). This is similar to the results of previous studies for all types of substitutions in $BaFe_2As_2$[39–43]. The response to irradiation in the x =0.25 sample is qualitatively different (bottom left panel of Fig. 2). While the superconducting

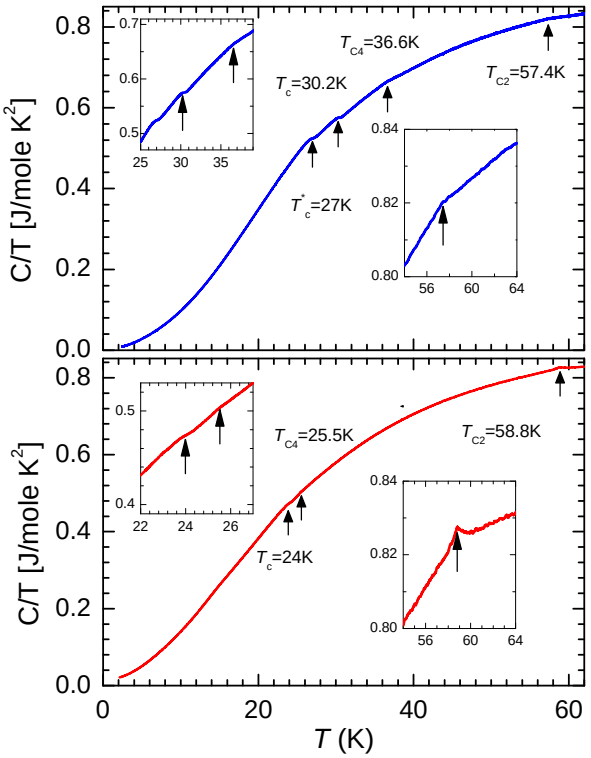

FIG. 3. (Color online) Temperature-dependent heat capacity, C/T, of $Ba_{1-x}K_xFe_2As_2$ sample x =0.25 before (top panel) and after (bottom panel) electron irradiation with 5.045 C/cm^2. Right insets zoom on T_{C2} phase transition, left insets on low-temperature transitions.

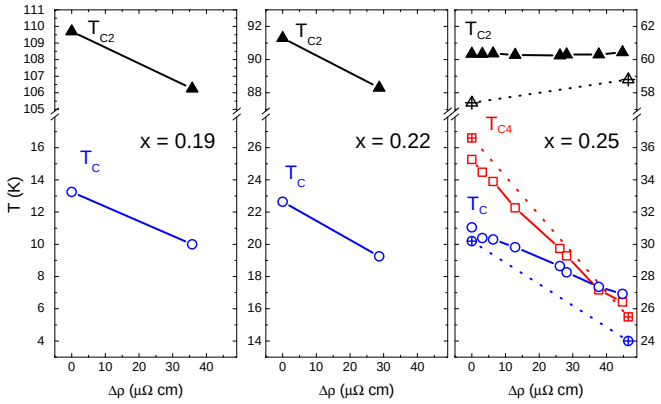

FIG. 4. (Color online) Transition temperatures of samples of $Ba_{1-x}K_xFe_2As_2$ x=0.19 (left panel), x=0.22 (center panel), and x=0.25 (right panel) as a function of scattering rate increase characterized with resistivity increase in the paramagnetic tetragonal phase above T_{C2}. Note the similar rates of superconducting T_c suppression in all compositions (blue open circles), the fast suppression of C_2 phase (black solid up-triangles) in samples x =0.19 and 0.22, the two times faster suppression of C_4 phase in x =0.25 (open red squares from resistivity measurements, crossed squares from heat capacity measurements), and the slight increase of T_{C2} with irradiation in x =0.25 (solid up-triangles resistivity measurements, crossed triangles from heat capacity measurements). Blue crossed circles are T_c from heat capacity measurements.

transition temperature is monotonically suppressed with increasing resistivity, the T_{C4} feature moves to lower temperatures significantly faster than T_c and eventually becomes indistinguishable from the superconducting transition. Furthermore, the T_{C2} feature is not suppressed with increasing scattering but, in fact, a slight increase of T_{C2} with irradiation is found in heat capacity measurements.

The findings in resistivity measurements are well matched by the heat capacity measurements. In the pristine state, top panel in Fig. 3, clear changes of slope are seen in the C/T vs T plot at T_{C2} =57.4 K, T_{C4} =36.6 K as well as two low-temperature features corresponding to the superconducting transition and possibly the reentrant C_2 phase. These features are shown with crossed symbols in Fig. 1 above. T_{C4} is strongly suppressed after irradiation, faster than the superconducting transition, while the C_2 transition becomes sharper and moves slightly up in temperature.

In Fig. 4 we summarize our observations as plots of characteristic temperatures for $Ba_{1-x}K_xFe_2As_2$ as a function of change of resistivity after irradiation. Left panel is data for the sample with x =0.19, middle panel for x =0.22 and right panel is for x =0.25. Note that the rates of the superconducting transition suppression with disorder, 0.091, 0.118 and 0.098 $K/\mu\Omega$cm for x=0.19, 0.22 and 0.25 respectively, are very close to each other and to the rate of the T_{C2} suppression, 0.096, and 0.105 for x =0.19 and x =0.22. The rate of the C_4 phase suppression in sample x =0.25, 0.21 $K/\mu\Omega$cm in resistivity and 0.24 $K/\mu\Omega$cm in heat capacity measurements, is about two times faster than that of C_2 phase suppression in x =0.19 and x =0.22 samples. This rate is also significantly higher than the rate of C_4 spin-vortex phase suppression in $CaK(Fe_{1-x}Ni_x)_4As_4$, 0.16 $K/\mu\Omega$cm[31]. A slight increase of T_{C2} in sample x =0.25 is found after irradiation in heat capacity measurements.

It is most natural to explain our findings as evidence for competition between the C_2 and the C_4 phases, with a suppression of the C_4 phase leading to a stabilization of the C_2 phase. Interestingly, this behavior is found for a certain parameter range in the calculations of Hoyer *et al.*[30,44], though this paper considers the case of phase competition near the magnetic transition temperature as opposed to the case of the C_4 phase existing deep in the domain of the C_2 phase as found in our experiment.

In conclusion, we find that controlled disorder introduced by low-temperature irradiation with relativistic 2.5 MeV electrons rapidly suppresses the transition temperature between antiferromagnetic C_2 and C_4 phases and leads to the relative stabilization of the C_2 phase. This behavior can be found for the parameter range characterized by weak nesting in the itinerant electron magnetism model by Hoyer *et al.*[30], though the phase stability relations were considered only at the transition temperature for magnetic ordering. Our findings suggest that further theoretical analysis that will consider possible 1st order

transition between two phases, hence, phase coexistence and possible separation, may be necessary.

We thank R. M. Fernandes, P. P. Orth and J. Schmalian for useful discussions. This work was supported by the Laboratory Directed Research and Development (LDRD) program of The Ames Laboratory, which is operated for the U.S. DOE by Iowa State University under contract # DE-AC02-07CH11358. We thank B. Boizot and all SIRIUS team for operating electron irradiation at SIRIUS facility at École Polytechnique [supported by the EMIR (Réseau national daccélérateurs pour les Études des Matériaux sous Irradiation) network, proposal 16-2125]. U.W. acknowledges funding from the U.S. Department of Energy, Office of Science, Basic Energy Sciences, Materials Sciences and Engineering Division. K.W. acknowledges support from the Swiss National Science Foundation through the Postdoc Mobility program.

[1] N. D. Mathur, F.M. Grosche, S. R. Julian, I. R. Walker, D. M. Freye, R. K.W. Haselwimmer, and G. G. Lonzarich, Nature (London) **394**, 39 (1998).
[2] B. D. White, J. D. Thompson, and M. B. Maple, Physica C- Supercond. and its applications, **514**, 246 (2015).
[3] B. Keimer, S. A. Kivelson, M. R. Norman, S. Uchida, and J. Zaanen, Nature(London) **518**, 179 (2015).
[4] Johnpierre Paglione, and Richard L. Greene, Nature Phys. **6**, 645 (2010).
[5] P. Monthoux, D. Pines, and G. G. Lonzarich, Nature (London) **450**, 1177 (2007).
[6] Hilbert von Lohneysen, Achim Rosch, Matthias Vojta, and Peter Wolfle, Rev. Mod. Phys. **79**, 1015 (2007).
[7] K. Kyuil Cho, M. Konczykowski, S. Teknowijoyo, M. A. Tanatar, J. Guss, P. B. Gartin, J. M. Wilde, A. Kreyssig, R. J. McQueeney, A. I. Goldman, V. Mishra, P. J. Hirschfeld, and R. Prozorov, Nature Comm. **9**, 2796 (2018).
[8] Y. Nakai, T. Iye, S. Kitagawa, K. Ishida, H. Ikeda, S. Kasahara, H. Shishido, T. Shibauchi, Y. Matsuda, and T. Terashima, Phys. Rev. Lett.**105**, 107003 (2010).
[9] M. A. Tanatar, K. Hashimoto, S. Kasahara, T. Shibauchi, Y. Matsuda, and R. Prozorov, Phys. Rev. B **87**, 104506 (2013).
[10] Ian M. Hayes, Ross D. McDonald, Nicolas P. Breznay, Toni Helm, Philip J. W. Moll, Mark Wartenbe, Arkady Shekhter, James G. Analytis, Nature Phys. **12**, 916 (2016).
[11] Clarina de la Cruz, Q. Huang, J. W. Lynn, Jiying Li, W. Ratcliff II, J. L. Zarestky, H. A. Mook, G. F. Chen, J. L. Luo, N. L. Wang, and Pengcheng Dai, Nature (London) **453**, 899 (2008).
[12] Marianne Rotter, Marcus Tegel, Dirk Johrendt, Inga Schellenberg, Wilfried Hermes, and Rainer Pttgen Phys. Rev. B **78**, 020503(R) (2008).
[13] E. Hassinger, G. Gredat, F. Valade, S. R. de Cotret, A. Juneau-Fecteau, J.-Ph. Reid, H. Kim, M. A. Tanatar, R. Prozorov, B. Shen, H.-H. Wen, N. Doiron-Leyraud, and Louis Taillefer Phys. Rev. B**86**, 140502(R) (2012).
[14] E. Hassinger, G. Gredat, F. Valade, S. Ren de Cotret, O. Cyr-Choinire, A. Juneau-Fecteau, J.-Ph. Reid, H. Kim, M. A. Tanatar, R. Prozorov, B. Shen, H.-H. Wen, N. Doiron-Leyraud, and Louis Taillefer Phys. Rev. B**93**, 144401 (2016).
[15] A. E. Böhmer, F. Hardy, L. Wang, T. Wolf, P.Schweiss, and C. Meingast, Nat. Comm. **6**, 7911 (2015).
[16] S. Avci, J. M. Allred, O. Chmaissem, D. Y. Chung, S. Rosenkranz, J. A. Schlueter, H. Claus, A. Daoud-Aladine, D. D. Khalyavin, P. Manuel, A. Llobet, M. R. Suchomel, M. G. Kanatzidis, and R. Osborn, Phys. Rev. B**88**, 094510 (2013).
[17] J. M. Allred, S. Avci, D. Y. Chung, H. Claus, D. D. Khalyavin, P. Manuel, K. M. Taddei, M. G. Kanatzidis, S. Rosenkranz, R. Osborn, and O. Chmaissem, Phys. Rev. B**92**, 094515 (2015).
[18] L. Wang, F. Hardy, A. E. Böhmer, T. Wolf, P. Schweiss, and C. Meingast, Phys. Rev. B**93**, 014514 (2016).
[19] Q.-P. Ding, W. R. Meier, J. Cui, M. Xu, A. E. Böhmer, S. L. Bud'ko, P. C. Canfield, and Y. Furukawa, Phys. Rev. Lett.**121**, 137204 (2018).
[20] K. M. Taddei, J. M. Allred, D. E. Bugaris, S. H. Lapidus, M. J. Krogstad, H. Claus, D. Y. Chung, M. G. Kanatzidis, R. Osborn, S. Rosenkranz, and O. Chmaissem, Phys. Rev. B**95**, 064508 (2017).
[21] K. M. Taddei, J. M. Allred, D. E. Bugaris, S. Lapidus, M. J. Krogstad, R. Stadel, H. Claus, D. Y. Chung, M. G. Kanatzidis, S. Rosenkranz, R. Osborn, and O. Chmaissem, Phys. Rev. B**93**, 134510 (2016)
[22] M. G. Kim, A. Kreyssig, A. Thaler, D. K. Pratt, W. Tian, J. L. Zarestky, M. A. Green, S. L. Budko, P. C. Canfield, R. J. McQueeney, and A. I. Goldman, Phys. Rev. B**82**, 220503(R) (2010).
[23] J. M. Allred, K. M. Taddei, D. E. Bugaris, M. J. Krogstad, S. H. Lapidus, D. Y. Chung, H. Claus, M. G. Kanatzidis, D. E. Brown, J. Kang, R. M. Fernandes, I. Eremin, S. Rosenkranz, O. Chmaissem, and R. Osborn, Nature Phys. **12**, 493 (2016).
[24] William R. Meier, Qing-Ping Ding, Andreas Kreyssig, Sergey L. Bud'ko, Aashish Sapkota, Karunakar Kothapalli, Vladislav Borisov, Roser Valenti, Cristian D. Batista, Peter P. Orth, Rafael M. Fernandes, Alan I. Goldman, Yuji Furukawa, Anna E. Böhmer, Paul C. Canfield, NPJ Quantum Materials **3**, 5 (2018).
[25] R. M. Fernandes, S. A. Kivelson, and E. Berg, Phys. Rev. B**93**, 014511 (2016).
[26] Jing Wang, Guo-Zhu Liu, Dmitry V. Efremov, and Jeroen van den Brink, Phys. Rev. B**95**, 024511 (2017).
[27] Rong Yu, Ming Yi, Benjamin A. Frandsen, Robert J. Birgeneau, Qimiao Si, arxiv.1706.07087
[28] Morten H. Christensen, Peter P. Orth, Brian M. Andersen, and Rafael M. Fernandes, Phys. Rev. B**98**, 014523 (2018).
[29] Morten H. Christensen, Peter P. Orth, Brian M. Andersen, and Rafael M. Fernandes, Phys. Rev. Lett.**121**, 057001 (2018).
[30] Mareike Hoyer, Rafael M. Fernandes, Alex Levchenko, and Jörg Schmalian, Phys. Rev. B**93**, 144414 (2016).
[31] S. Teknowijoyo, K. Cho, M. Koczykowski, E. I. Timmons, M. A. Tanatar, W. R. Meier, M. Xu, S. L. Bud'ko, P. C. Canfield, and R. Prozorov, Phys. Rev. B**97**, 140508(R) (2018).

[32] Y. Liu, M. A. Tanatar, W. E. Straszheim, B. Jensen, K. W. Dennis, R. W. McCallum, V. G. Kogan, R. Prozorov, and T. A. Lograsso, Phys. Rev. B**89**, 134504 (2014).
[33] M. A. Tanatar, N. Ni, S. L. Bud'ko, P. C. Canfield, and R. Prozorov, Supercond. Sci. Technol. **23**, 054002 (2010).
[34] M. A.Tanatar, R. Prozorov, N. Ni, S. L. Bud'ko, P. C. Canfield, U.S. Patent 8,450,246 (Sept.1, 2011).
[35] S. Tagliati, V. M. Krasnov, and A. Rydh, Rev. Sci. Instrum. **83**, 055107 (2012).
[36] K. Willa, S. Diao, D. Campanini, U. Welp, R. Divan, M. Hudl, Z. Islam, W.-K. Kwok, and A. Rydh, Rev. Sci. Instrum. **88**, 125108 (2017).
[37] http://emir.in2p3.fr/ LSI, electron irradiation facility.
[38] M. A. Tanatar, W. E. Straszheim, Hyunsoo Kim, J. Murphy, N. Spyrison, E. C. Blomberg, K. Cho, J.-Ph. Reid, Bing Shen, Louis Taillefer, Hai-Hu Wen, and R. Prozorov, Phys. Rev. B**89**, 144514 (2014).
[39] Yuta Mizukami, Marcin Konczykowski, Kohei Matsuura, Tatsuya Watashige, Shigeru Kasahara, Yuji Matsuda, and Takasada Shibauchi, J. Phys. Soc. Jpn **86**, 083706 (2017).
[40] L. Liu, T. Mikami, S. Ishida, K. Koshiishi, K. Okazaki, T. Yoshida, H. Suzuki, M. Horio, L. C. C. Ambolode, II, J. Xu, H. Kumigashira, K. Ono, M. Nakajima, K. Kihou, C. H. Lee, A. Iyo, H. Eisaki, T. Kakeshita, S. Uchida, and A. Fujimori, Phys. Rev. B92, 094503 (2015).
[41] E. C. Blomberg, M. A. Tanatar, A. Thaler, S. L. Bud'ko, P. C. Canfield, and R. Prozorov, J. Phys. Cond. Matt. **30**, 315601 (2018).
[42] K. Cho, M. Kończykowski, J. Murphy, H. Kim, M. A. Tanatar, W. E. Straszheim, B. Shen, H. H. Wen, and R. Prozorov, Phys. Rev. B**90**, 104514 (2014).
[43] R. Prozorov, M. Konczykowski, M. A. Tanatar, H. H. Wen, R. M. Fernandes, P. C. Canfield, arXiv:1808.09532
[44] This can be seen most clearly as a slight expansion of the (green, SM) domain of C_2 phase in the central area of Fig. 2 in the paper by Hoyer *et al.*,[30].